



HAL
open science

Monitoring recovery after CNS demyelination, a novel tool to de-risk pro-remyelinating strategies

Esther Henriët, Elodie M Martin, Pauline Jubin, Dominique Langui, Abdelkrim Mannioui, Bruno Stankoff, Catherine Lubetzki, Arseny Khakhalin, Bernard Zalc

► To cite this version:

Esther Henriët, Elodie M Martin, Pauline Jubin, Dominique Langui, Abdelkrim Mannioui, et al.. Monitoring recovery after CNS demyelination, a novel tool to de-risk pro-remyelinating strategies. Brain - A Journal of Neurology , 2023, 10.1093/brain/awad051 . hal-04056916

HAL Id: hal-04056916

<https://hal.sorbonne-universite.fr/hal-04056916>



Submitted on 7 Apr 2023

HAL is a multi-disciplinary open access archive for the deposit and dissemination of scientific research documents, whether they are published or not. The documents may come from teaching and research institutions in France or abroad, or from public or private research centers.

L'archive ouverte pluridisciplinaire **HAL**, est destinée au dépôt et à la diffusion de documents scientifiques de niveau recherche, publiés ou non, émanant des établissements d'enseignement et de recherche français ou étrangers, des laboratoires publics ou privés.



Monitoring recovery after CNS demyelination, a novel tool to de-risk pro-remyelinating strategies

Esther Henriët,^{1,†} Elodie M. Martin,^{1,†} Pauline Jubin,^{1,†} Dominique Langui,¹ Abdelkrim Mannioui,¹  Bruno Stankoff,^{1,2} Catherine Lubetzki,^{1,3} Arseny Khakhalin⁴ and  Bernard Zalc¹

[†]These authors contributed equally to this work.

In multiple sclerosis, while remarkable progress has been accomplished to control the inflammatory component of the disease, repair of demyelinated lesions is still an unmet need. Despite encouraging results generated in experimental models, several candidates favouring or promoting remyelination have not reached the expected outcomes in clinical trials. One possible reason for these failures is that, in most cases, during preclinical testing, efficacy was evaluated on histology only, while functional recovery had not been assessed.

We have generated a *Xenopus laevis* transgenic model Tg(*mbp*:GFP-NTR) of conditional demyelination in which spontaneous remyelination can be accelerated using candidate molecules. *Xenopus laevis* is a classic model for *in vivo* studies of myelination because tadpoles are translucent. We reasoned that demyelination should translate into loss of sensorimotor functions followed by behavioural recovery upon remyelination. To this end, we measured the swimming speed and distance travelled before and after demyelination and during the ongoing spontaneous remyelination and have developed a functional assay based on the visual avoidance of a virtual collision.

Here we show that alteration of these functional and clinical performances correlated well with the level of demyelination and that histological remyelination, assayed by counting *in vivo* the number of myelinating oligodendrocytes in the optic nerve, translated in clinical–functional recovery. This method was further validated in tadpoles treated with pro-remyelinating agents (clemastine, siponimod) showing that increased remyelination in the optic nerve was associated with functional improvement.

Our data illustrate the potential interest of correlating histopathological parameters and functional–clinical parameters to screen molecules promoting remyelination in a simple *in vivo* model of conditional demyelination.

1 Sorbonne Université, Inserm, CNRS, ICM-GH Pitié-Salpêtrière, F-75013 Paris, France

2 AP-HP, Saint-Antoine Hospital, F-75012 Paris, France

3 AP-HP, GH Pitié-Salpêtrière, F-75013 Paris, France

4 Bard College, 30 Campus Rd, Annandale-on-Hudson, NY 12504, USA

Correspondence to: B. Zalc

Sorbonne Université, Inserm, CNRS

ICM-GH Pitié-Salpêtrière, Bvd de l'Hôpital, F-75013 Paris, France

E-mail: bernard.zalc@upmc.fr

Keywords: *Xenopus*; visual system; optic nerve; myelin; regeneration

Received April 04, 2022. Revised December 15, 2022. Accepted January 22, 2023. Advance access publication March 30, 2023

© The Author(s) 2023. Published by Oxford University Press on behalf of the Guarantors of Brain.

This is an Open Access article distributed under the terms of the Creative Commons Attribution-NonCommercial License (<https://creativecommons.org/licenses/by-nc/4.0/>), which permits non-commercial re-use, distribution, and reproduction in any medium, provided the original work is properly cited. For commercial re-use, please contact journals.permissions@oup.com

Introduction

Myelin, synthesized by oligodendrocytes in the CNS and Schwann cells in the peripheral nervous system, consists of a membrane spirally wrapped around large axons—with a diameter usually larger than $0.5\ \mu\text{m}$ ¹—forming a sheath, which is interrupted at more or less regular spacing, known as nodes of Ranvier. It was Louis Ranvier who initially proposed that the function of myelin was to protect and separate the axons from their surroundings.² In myelinated axons voltage-gated sodium channels (Na_v) are aggregated at the nodes of Ranvier and the action potential ‘jumps’ from one node to the next, a mode of propagation known as saltatory conduction, which allows a 50- to 100-fold acceleration of propagation of the action potential along the axon. Neurons rely on their myelinating partners not only for setting conduction speed, but also for regulating the ionic environment and fuelling their energy demands with metabolites. Indeed, another function of the myelin sheath is to provide nutrients, mostly lactate, to the axon along the length of the axon.^{3,4}

Demyelination in CNS diseases, including multiple sclerosis, alters axonal function and can result in permanent disability. Myelin loss around axons leads to slowing down of nerve conduction and even to conduction block when several adjacent internodes are demyelinated, and finally to degeneration of denuded axons and neuronal loss. These neuropathological features translate into clinical signs, such as paraparesis, paralysis or sensory deficit and finally irreversible neurological disability.⁵ Despite an important array of experimental models mostly developed in rodents, the precise link between a given demyelinated lesion and a definite sensorimotor deficit is often missing.

To investigate myelin formation and remyelination, we have generated a *Xenopus laevis* transgenic line allowing conditional ablation of myelinating oligodendrocytes. In this Tg(*mbp*:GFP-NTR) transgenic line, the green fluorescent protein (GFP) reporter fused to *Escherichia coli* nitroreductase (NTR) is expressed specifically in myelinating oligodendrocytes. Nitroreductase converts the innocuous pro-drug metronidazole (MTZ) to a cytotoxin. To induce conditional demyelination, MTZ is introduced into the aquarium water and withdrawal of MTZ leads to spontaneous remyelination. As tadpoles are transparent, these events can be monitored *in vivo* and quantified.⁶ Due to optical accessibility, we focused on the optic nerve. We confirmed that counting the number of GFP+ cells per optic nerve is a reliable indicator of the extent of demyelination and remyelination by electron microscopy analysis. Furthermore, to ascertain that demyelination translates into loss of sensorimotor functions we adapted a virtual collision visual avoidance paradigm in *Xenopus* tadpole^{7,8} to test the behavioural consequence of demyelination and the return to normal after spontaneous remyelination. Quantitative evaluation of behavioural perturbation was confronted to the degree of demyelination–remyelination assayed by counting the number of GFP+ oligodendrocytes.

Materials and methods

Animals

All experiments were performed on stage 50–52 *X. laevis* tadpoles staged according to Nieuwkoop and Faber normal tables.⁹ Animals were obtained following injection of pairs of adults, selected from our colony of either transgenic Tg(*mbp*:GFP-NTR)⁶ or wild-type raised in our animal facility (agreement # A75-13-19), with human

chorionic gonadotrophin (1000 i.u./ml; Sigma-Aldrich). Eggs were collected and reared in trays at temperatures between 20 and 23°C until they had reached the desired development stage, after 15–25 days. Tadpoles of either sex were anaesthetized in 0.05% MS-222 (ethyl-3-aminobenzoate methanesulphonate; Cayman Chemical) before quantification of GFP+ cells and returned to normal water to recover. Before brain and spinal cord dissection, tadpoles were euthanized in 0.5% MS-222. Stages NF50–NF55 correspond to pre-metamorphosis and represent stages in which myelination is ongoing (see <https://www.xenbase.org/entry/anatomy/alldev.do>). In the optic nerve at the EM level, myelination begins in the middle portion at stage NF48/49 and the number of myelinated axons increases 7-fold between stages 50 and 57.¹⁰

Animal care was in accordance with institutional and national guidelines. All animal procedures conformed to the European Community Council 1986 directive (86/609/EEC) as modified in 2010 (2010/603/UE) and have been approved by the ethical committee of the French Ministry of Higher Education and Research (APAFIS#5842-2016101312021965).

Metronidazole preparation and use

Metronidazole (Sigma Aldrich) was dissolved in filtered tap water containing 0.1% dimethyl sulphoxide (DMSO; Sigma Aldrich). MTZ was used at concentration of 10 mM with an exposure length of 10 days. Transgenic or non-transgenic sibling tadpoles were maintained in 600 ml of MTZ solution (maximum 10 tadpoles/600 ml) at 20°C in complete darkness (MTZ is light-sensitive) and the solution was changed every other day throughout the duration of treatment. For regeneration experiments, MTZ-exposed animals were allowed to recover for 3 and 8 days in normal water in ambient laboratory lighting (12 h light/12 h dark).

Antibodies

For double or triple immune labelling the following antibodies were used: rabbit anti-GFP (1:500; InVitrogen), rabbit anti-pan neurofascin (NFC2; 1:500; a generous gift of Dr P. Brophy),¹¹ chicken anti-myelin basic protein (MBP; 1:500; Millipore); mouse Mab IgG1 anti-neurofilament, clone 3A10 (1:500) was from Developmental Studies Hybridoma Bank, Iowa City, IA. Alexa fluorescent secondary antibodies were from InVitrogen (ThermoFisher Scientific) and all were used at a dilution of 1/1000.

Immunolabelling

Whole-mount immunolabelling of optic nerve

Fixed tadpole optic nerves were carefully dissected and rinsed in Triton® X-100 [0.3% in phosphate buffer saline (PBS) 1× = PBT 0.3%] for 1 h with change in PBT 0.3% every 15 min. Samples were then incubated in blocking solution [normal goat serum (Thermoscientific) diluted 5% in PBT 0.3%] for 2 h. Anti-GFP antibody was added in the blocking solution and incubated overnight on a gentle shaker at 4°C. The primary antibody was removed and rinsed for 2 h in PBT 0.1%, with changes every 15 min. Secondary antibody was used in blocking solution and incubated 2 h at room temperature on a gentle rotating shaker. The secondary antibody was removed and the labelled optic nerves rinsed in PBT 0.1% for 2 h with changes every 15 min. DAPI (InVitrogen) was used to label the nuclei and rinsed in PBT 0.1% for 5 min and mounted on a glass slide in tissue-clearing solution (RapiClear 1.49 medium, Nikon).

Immunohistochemistry

Dissected tadpole brains were fixed by immersion in 4% paraformaldehyde rinsed in PBS (1×) and cryoprotected in sucrose (20% in PBS). Cryoprotected brains were embedded in OCT® (Tissue Tek). Horizontal cryosections (16 µm thick) were blocked in normal goat serum (5% in PBS) containing 0.1% Triton® X-100 and incubated overnight at 4°C with primary antibodies. Slides were rinsed in PBT 0.1% and secondary antibody added. The slides were mounted with DAPI-coated Vectashield antifade mounting medium® (Vectorlabs).

Electron microscopy

Larvae were fixed in a mixture of 2% paraformaldehyde, 2% glutaraldehyde, in 0.1 M cacodylate buffer pH 7.4% and 0.002% calcium chloride overnight at 4°C, washed in 0.1 M cacodylate buffer and postfixed in 1% osmium tetroxide, 1% potassium ferricyanide in 0.1 M cacodylate buffer. After washing in cacodylate buffer and water, larvae were incubated in 2% uranyl acetate aqueous solution at 4°C overnight. After rinsing twice in water, larvae were dehydrated in increasing concentrations of ethanol, with the final dehydration in 100% acetone (twice, 10 min each). Samples were infiltrated with 50% acetone 50% Epon for 2 h and then embedded in Epon (EMBed 812, Electron Microscopy Sciences Cat 14 120). Blocks were heated at 56°C for 48 h. Ultrathin sections (70 nm) were examined on an HT7700 electron microscope (Hitachi) operated at 70 kV.

Quantification of myelinated axons

The number of myelinated axons per optic nerve and brain stem was determined on coronal semi-thin sections 0.5 µm thick. Sections were stained with toluidine blue for 5 min. Images were acquired at ×63 or ×100 magnification. Quantification in the optic nerve was performed at D0, D10, R3 and R8 and three nerves were counted for each stage. Evaluation of MTZ-induced demyelination in the brain stem was at D10; on average, 10–12 sections of 5–6 animals were counted.

Quantification of GFP+ cells

GFP was detected directly by fluorescence in live MBP-GFP-NTR transgenic *Xenopus* embryos using an AZ100 Nikon Zoom Macroscope. The total number of GFP+ cells was counted in the optic nerve, from the emergence of the nerve (i.e. after the chiasm) to the retinal end. For stage 50 tadpoles the length of the optic nerve is on average 1700 µm ± 100 µm for a diameter of 50 µm. GFP+ cells were counted before (D0) and at the end of MTZ exposure (D10) and after being returned to normal water for either 3 or 8 days (R3 or R8, respectively) or water containing the molecule to be tested on the same embryos. The following molecules were used: clemastine (200 nM; clemastine fumarate salt, SML0445, Sigma Aldrich), siponimod (3 nM; Abmole M2428 BAF312), siramesine (5 µM; SML0976, Sigma Aldrich) and sildenafil (1 µM; S4684, Selleckchem). Counts were performed independently by two researchers. Difference in numbers obtained by each researcher was below 10%. Data were compared to control untreated animals of the same developmental stage.

Behavioural testing

Tadpoles were tested in the morning before being fed. The setup consists of a CRT monitor (Dell Model #M570, 100–240 V, 60/50 Hz, 1.4 A, refresh rate used 60 Hz). The screen was covered with a 10 mm diameter mask, adapted to a Petri dish. Movements of tadpoles were recorded with a Dragonfly2 DR2-HIBW camera at 30

pfs and the Computar M3Z1228C-MP2/3' 12–36 mm Varifocal, Manual Iris Megapixel (C mount) lens. The video recording system used was FlyCapture2 (Supplementary Fig. 2).

The setup was localized in a darkroom; the light was turned off so that the only light perceived by tadpoles came from the screen. Each animal was tested separately in the Petri dish filled up to 1 cm with MMR 0.1 X medium. Tadpoles were placed in the Petri dish and left to adapt to the screen light for 5–10 s. Spontaneous swimming was recorded for 30 s and average speed for this period analysed. If the animal was immobile at first it was touched with a plastic pipette to initiate movement, this first acceleration being excluded from analysis.

The virtual avoidance collision test was performed after all animals had been tested for spontaneous swimming behaviour. A black dot (18 pixel = 8 mm on the screen) was presented on the screen, the experimenter targeted the eye of the tadpole by changing the direction and speed of the dot. On average, 5–6 try outs were performed to assess visual avoidance. The virtual collision setup can be found on the AK website <https://github.com/khakhalin/Xenopus-Behavior>.

Analysis of videos recordings was with Noldus Ethovision XT 11.5 software. For each experiment detection settings were calibrated. After tracking of the tadpole and the moving black dot the trajectories were individually verified and modified in case of swapping identity between tadpole and dot or in case of failure of automated detection. To determine visual avoidance several escape responses were analysed and it was determined that a successful avoidance response corresponded to an acceleration swim of the tadpole >50 cm/s² and a change in direction (C-start) verified by the experimenter, initiated for a distance between the tadpole and the dot of 1–1.3 cm. Data are presented as an avoidance rate, i.e. the ratio of the number of encounters that resulted in a successful avoidance.

Statistical analysis

We used Prism GraphPad software (GraphPad Prism version 8) for statistical analyses. Data presented are the mean ± SEM of number of GFP+ cells counted on at least 16 tadpoles per condition. For the analysis of two groups, an unpaired two-tailed Student t-test or a Mann–Whitney test were applied. For more than two group analyses, a one-way ANOVA with Tukey's multiple comparison test or a Kruskal–Wallis with Dunn's multiple comparisons test were applied. Statistical significance was defined as *P < 0.05, **P < 0.01 and ***P < 0.001.

Data availability

All data are available upon reasonable request. Data supporting this article are given in the text and [Supplementary material](#).

Results

Description of the Tg(*mbp*:GFP-NTR) *Xenopus* model

When planning our transgenic construct to drive the expression of the GFP-NTR transgene into myelin-forming oligodendrocytes, the 1.9 kb proximal portion of mouse MBP regulatory sequence was chosen. We had previously shown that this portion of mouse DNA upstream of the ATG start codon of MBP contains sequences restricting the expression of reporter transgene to mature myelin-forming oligodendrocytes.¹² Within this 1.9 kb non-coding sequence the initial 256 bp of MBP non-coding sequence is highly

conserved between human and mouse¹³ and comparison between mouse and *X. laevis* show 81% homology and 49 mismatches (<<http://www.xenbase.org/genomes/blastSeq.do>>). In the Tg(*mbp:GFP-NTR*) *Xenopus* line, similar to the observation in the 1.9 kb Tg(*mbp:lacZ*) transgenic mouse,¹⁴ the transgene is expressed only in myelin-forming oligodendrocytes, but not in cells earlier in the oligodendroglial lineage [oligodendrocyte precursor cells (OPCs) are Sox10+/GFP-; see figure 3 in Mannioui et al.¹⁵].

Metronidazole-induced demyelination

Our transgene construct is formed by the fusion of GFP with the *E. coli* NTR. This enzyme, absent from vertebrates, reduces nitro residues of compounds such as metronidazole (nitro-imidazol), into a highly toxic hydroxylamine derivative, [2-(5-(hydroxyamino)-2-methyl-1H-imidazol-1-yl)-ethanol]. Therefore, addition of metronidazole into the swimming water of Tg(*mbp:GFP-NTR*) tadpoles induces a dramatic cell death of cells expressing the transgene, which in our transgenic line are the myelin forming oligodendrocytes. Thanks to the transparency of *Xenopus* tadpoles, oligodendrocyte depletion during metronidazole exposure can be monitored on live animals (Fig. 1A–E). We have previously shown that the extent of oligodendrocyte ablation depends on metronidazole concentration and duration of exposure, which we routinely set as 10 mM for 10 days, resulting in the average between 75% and 90% depletion in the number of oligodendrocytes in the optic nerve.^{6,15}

Although oligodendrocyte cell death is ubiquitous, quantification was better performed in the optic nerve because this anatomical structure is more easily identified, allowing precise counting between the nerve exit at the papilla of the eye bulb (retinal portion) and its entry into the diencephalon (chiasmatic extremity; Fig. 1B–E). In stage NF50–52 (i.e. 25 days post-fertilization), Tg(*mbp:GFP-NTR*) transgenic tadpoles treated for 10 days with metronidazole (10 mM) show a decreased number of GFP+ cells per optic nerve from 21.0 ± 1.2 down to 2.7 ± 0.3 (D0, $n = 62$, D10, $n = 43$, $P < 0.001$; Fig. 1J). As expected from previous experiments, ablation of myelin-forming oligodendrocytes resulted in an extensive demyelination, which was verified by electron microscopy in the optic nerve of stages 50–52 Tg(*mbp:GFP-NTR*) transgenic tadpoles, showing the vast disappearance of myelinated axons (compare Fig. 1F and G). These data were strengthened by western blot of total brain extract probed with anti-MBP antibodies showing a clear decrease of the MBP signal at D10 (Supplementary Fig. 1). Quantification of extent of demyelination was performed on semi-thin sections by counting the number of myelinated axons [109 ± 12.6 before (D0) and at the end of metronidazole exposure (D10) (28.3 ± 1.2 ; $n = 3$ $m \pm$ SEM; Fig. 1K).

Spontaneous remyelination

At the end of 10 days exposure to MTZ the tadpoles were returned to normal water. The number of GFP+ oligodendrocytes per optic nerve reached 8.7 ± 0.9 ($n = 27$) and 15.3 ± 0.6 ($n = 16$) at 3 and 8 days of recovery, respectively (Fig. 1D, E and J). The number of myelinated axons on semi-thin sections of optic nerve was restored after 3 (R3) and 8 (R8) days of recovery (131 ± 7.7 and 138 ± 21.5 , respectively; $n = 3$ $m \pm$ SEM; Fig. 1H, I and K). The ratio of number of oligodendrocytes to axons was 5.1 on D0 and 9.0 on R8. Analysis of the g-ratio showed that at R3 myelin was significantly thinner than at D0 (0.8694 ± 0.0032 and 0.8943 ± 0.0035 for D0 and R3, respectively). At R8 although myelin thickness had notably improved ($g = 0.8832 \pm 0.0026$), myelin was still thinner than prior to demyelination (Fig. 1L).

Effect of demyelination and remyelination on swimming behaviour

We then assessed the behavioural sensorimotor consequences of demyelination and myelin regeneration. To this end we measured the swimming speed and distance travelled before and after demyelination and during the ongoing spontaneous remyelination. Each tadpole was placed in the Petri dish above the CRT monitor (Supplementary Fig. 2) and left to adapt to the light for 5–10 s before recording the swimming behaviour for 30 s (Fig. 2A and B and Supplementary Video 1). After 10 days in MTZ (10 mM) demyelinated animals swam a shorter distance than before demyelination: 87.7 ± 4.6 cm versus 55.6 ± 2.1 cm at D0 and D10, respectively (mean \pm SEM, $n = 75$; $P = 0.0081$; Fig. 2A, C and D and Supplementary Video 2). Similarly, the average speed of swimming of Tg(*mbp:GFP-NTR*) tadpoles (3.18 ± 0.15 cm/s) was significantly decreased at the end of the demyelination treatment (1.99 ± 0.06 cm/s; $m \pm$ SEM, $n = 75$; $P = 0.001$; Fig. 2C and E and Supplementary Video 2). To verify that alteration in swimming behaviour was not the consequence of introduction of MTZ in the medium, wild-type (WT) tadpoles were exposed to MTZ (10 mM). Ten days MTZ treatment of WT tadpoles had no significant effect either on the distance travelled [73.4 ± 9.8 cm versus 59.4 ± 7.3 cm ($P = 0.42$)] or on the average speed [2.2 ± 0.3 cm/s versus 2.8 ± 0.3 cm/s ($P = 0.22$; $n = 19$ WT versus $n = 23$ Tg(*mbp:GFP-NTR*)].

At R3, despite the increase of the number of both GFP+ cells and myelinated axons (measured in the optic nerve; Fig. 1J and K), the average speed and the distance travelled over a period of 30 s did not improve (distance: 50.7 ± 7.8 cm; speed: 1.72 ± 0.26 cm/s; $n = 41$). However, at R8 both parameters had returned to control levels before demyelination (distance: 83.6 ± 15.6 cm; speed: 2.88 ± 0.53 cm/s; $n = 13$; Fig. 2D and E).

Effect of demyelination and remyelination on a visual avoidance test

What are the functional consequences of the demyelination of the optic nerve? Does this extensive demyelination translate into a loss of vision similar to what is observed in multiple sclerosis patients with optic neuritis? To address this question we set up a visual avoidance test, which is based on the principle that if tadpoles have a normal vision they will avoid collisions with a projected black dot.^{8,16} Tadpoles swimming freely in a Petri dish positioned on top of a CRT monitor are confronted with an approaching black dot shown on the screen (Supplementary Fig. 2). It has been shown that visual avoidance response of tadpoles is characterized by a sharp turn (C-start) and acceleration (71.8 ± 4.1 cm/s²) to avoid the approaching moving dot^{7,17} (Fig. 3A and Supplementary Video 3). Because this visual avoidance behaviour involves the retino-tectal projection we predict that it may be altered following demyelination of the optic nerve.

In a first series of experiments we observed that not every tadpole avoided the black dot when it was presented on the screen. We therefore adjusted some parameters to increase the responsiveness of the tadpoles. Timing of feeding was one criterion; tadpoles fed just before the test had an average avoidance index of 0.09, compared to 0.51 for tadpoles fed the evening before ($P = 0.008$, $n = 10$). Tadpoles tested in the morning had a better response rate in the visual avoidance than in the afternoon, 0.63 versus 0.29, respectively ($P = 0.031$, $n = 7$). To test the reproducibility of the response stage 50–52 tadpoles were submitted daily for 10 days to the collision avoidance paradigm. Tadpoles that initially avoided the virtual collision continue to avoid it for the period tested, whereas those unresponsive

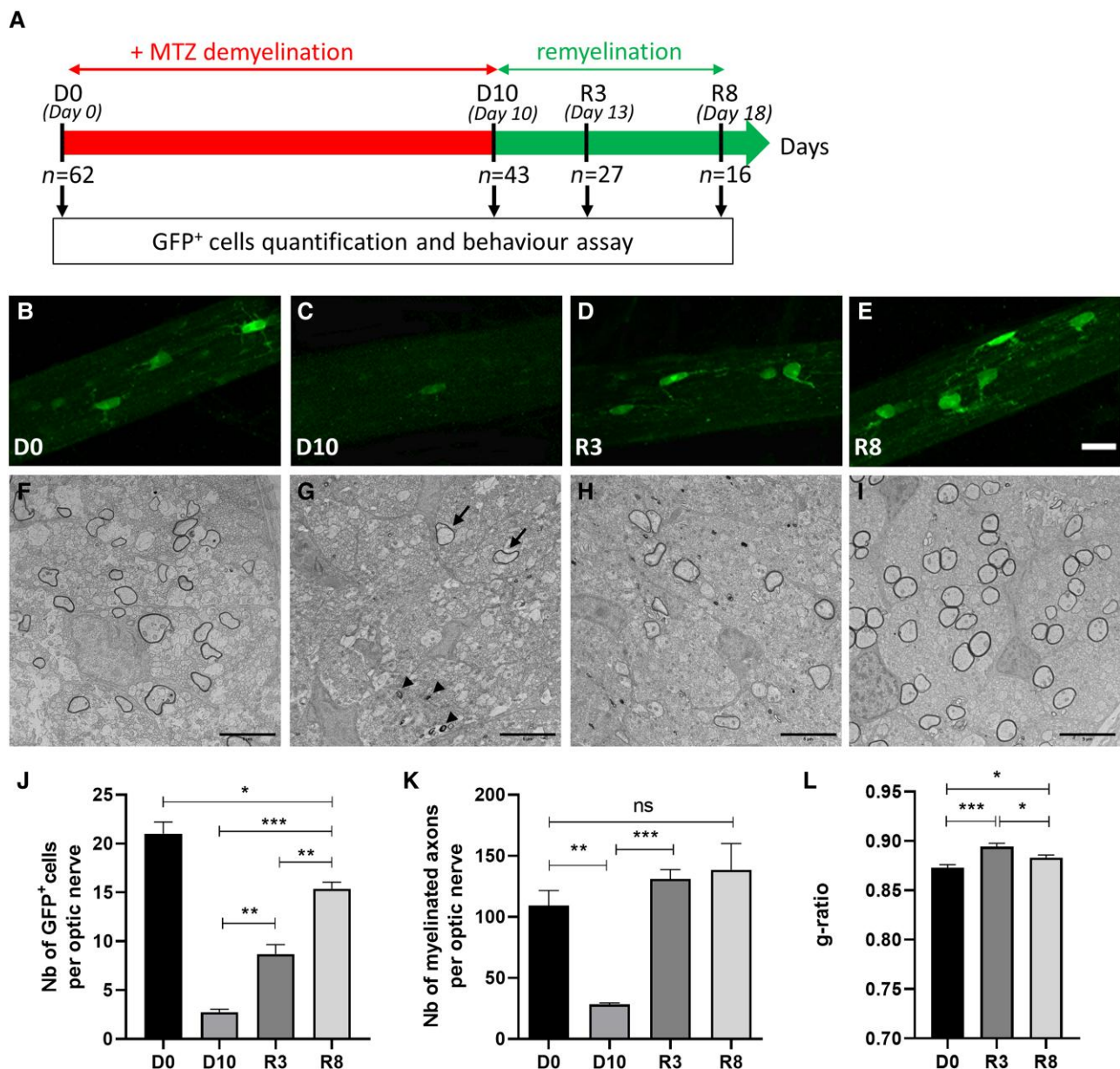


Figure 1 Confocal and electron microscopic illustration of conditional demyelination and spontaneous remyelination of *tg(mbp:GFP-NTR)* transgenic *X. laevis*. (A) Flow chart showing the sequence of events tested and the number of tadpoles throughout the experiment. (B–E) Optic nerve of *Tg(mbp:GFP-NTR)* *X. laevis* (stage 50 tadpole) before (D0), at the end of metronidazole exposure (D10) and after 3 days (R3) and 8 days (R8) spontaneous recovery; scale bar = 20 μ m. (F–I) Electron micrographs of transversal ultrathin sections (70 nm) of optic nerve of transgenic *Tg(mbp:GFP-NTR)* *X. laevis* tadpole before (F), at the end of metronidazole exposure (G) and after 3 days (H) and 8 days (I) of spontaneous recovery; in G arrows point to two axons that resisted MTZ-induced demyelination and arrowheads point to myelin debris; scale bar = 5 μ m. (J) Quantification of the number of GFP⁺ oligodendrocytes per optic nerve. (K) Quantification of myelinated axons counted on optic nerve semi-thin (0.5 μ m) sections stained with toluidine blue between D0 and R8. (L) Evolution of g-ratio measured on D0, R3 and R8. Data are expressed as mean \pm SEM (in K and L, $n = 3$ –4 tadpoles per group), with ** $P < 0.01$, *** $P < 0.001$ and **** $P < 0.0001$ calculated using an unpaired two-tailed Student's t-test between two groups with a 95% confidence interval.

in the initial test remained non-responsive. Therefore, this prompted us to select ‘responders’ tadpoles before starting the demyelination–remyelination experiment. On average, $47.9\% \pm 4.5\%$ tadpoles at stage 50–52 ($n = 222$) avoided the projected black dot more than 50% of the time. As a consequence, when planning a behaviour experiment we always test twice more tadpoles than the number necessary to achieve the experiment. Having set these parameters, animals were tested on D0, at the end of the MTZ-induced demyelination treatment (D10), then 3 and 8 days after stopping MTZ exposure (R3 and R8, respectively). At the end

of the demyelination period, tadpoles had lost the capability to avoid the threatening stimulus represented by the virtual collision with the black dot (compare Fig. 3A and B and Supplementary Videos 3 and 4). The avoidance index measured at D0 significantly decreased after 10 days of demyelination from 0.4 ± 0.04 to 0.16 ± 0.02 ; $n = 74$ (mean \pm SEM; $P < 0.0001$; Fig. 3C). To test whether this sharp decrease in the avoidance rate was not a consequence of an alteration of the swimming behaviour (see below) we verified that demyelinated animals were still responding to a touch reflex by submitting them to a touch stimulus with a plastic pipette

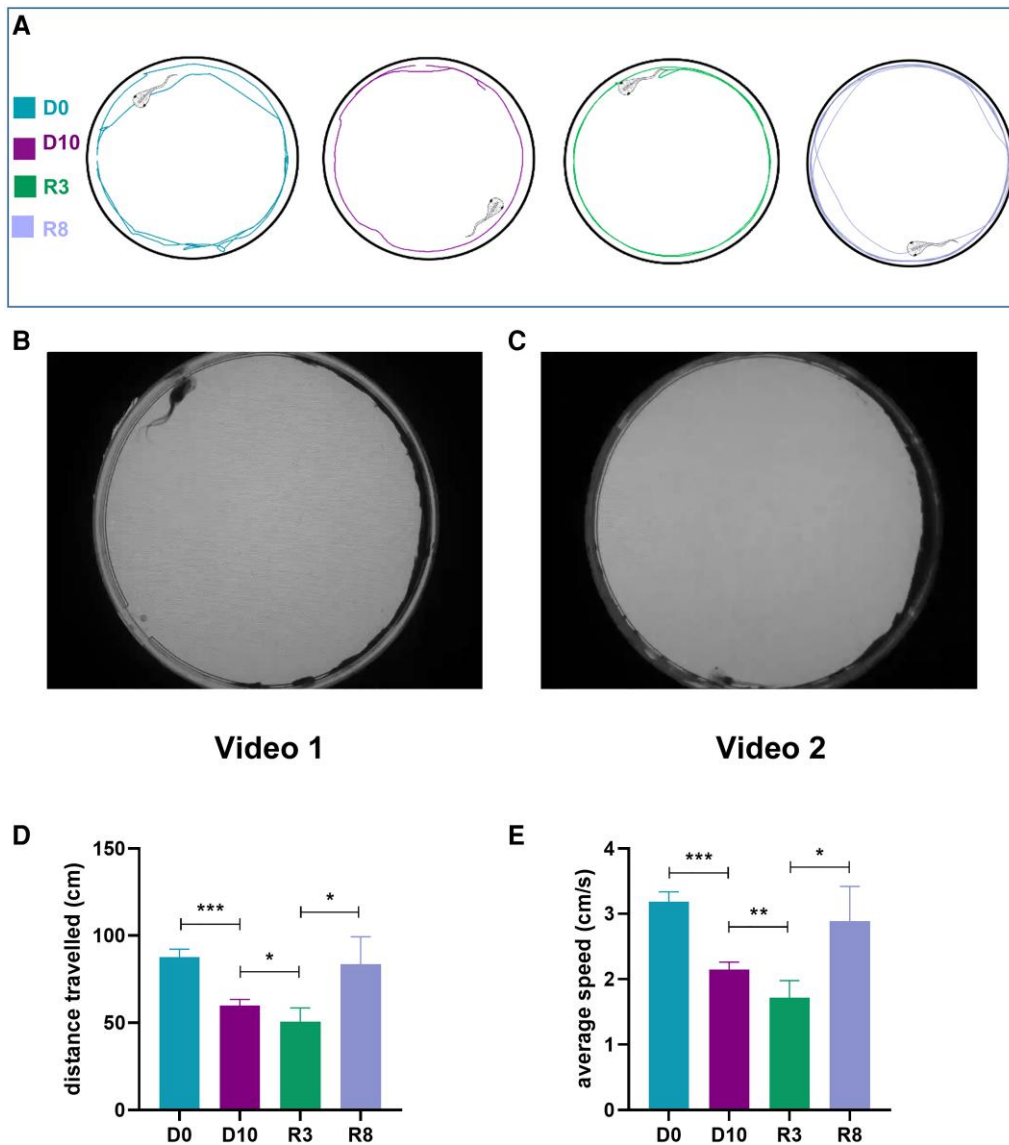


Figure 2 Swimming behaviour of *Tg(mbp:GFP-NTR)*. (A) Traces of distance swam recorded for a period of 30 s on D0, D10 and during the recovery period on R3 and R8. (B and C) Live imaging of the swimming behaviour of a tadpole before demyelination (See [Supplementary Video 1](#)) and after 10 days of exposure to MTZ (see [Supplementary Video 2](#)). (D and E) Average distance expressed in cm (D) and speed of swimming in cm/s (E) before ($n = 62$) and at the end of MTZ treatment ($n = 43$) and during the recovery period R3 ($n = 27$) and R8 ($n = 13$). Note that on R3, despite the partial increase in the number of GFP+ cells per optic nerve ([Fig. 1](#)), tadpoles did not improve their performance; however, the recovery was complete on R8.

([Supplementary Video 4](#) at 22 s). Three and 8 days after MTZ exposure was stopped, animals recovered rapidly with avoidance index of 0.27 ± 0.03 and 0.42 ± 0.07 at R3 ($n = 27$) and R8 ($n = 13$) (mean \pm SEM), respectively ([Fig. 3C](#)).

Demyelination consequence on the G-type startle response

The ability to detect a threatening stimulus, such as illustrated here by the virtual collision with a black dot initiating an escape response is essential for survival and is driven by a small reticulo-spinal network.^{18,19} Demyelination was quantified on transversal semi-thin sections stained with toluidine blue ([Supplementary Fig. 3](#)) showing that at the end of MTZ exposure the number of myelinated axons had decreased from $25.8 \pm 11.3/1000 \mu\text{m}^2$ (mean \pm SEM; $n = 5$) in control WT animals down to $12.8 \pm 3.8/1000 \mu\text{m}^2$ in *Tg(mbp:GFP-NTR)*

(mean \pm SEM; $n = 6$). However, demyelinated axons were not homogeneously distributed. Mauthner axons as well as axons in their vicinity, i.e. on the medio-dorsal portion of the transversal section, were still myelinated, suggesting they were more resistant to the MTZ exposure compared to the latero-ventral axons ([Fig. 4](#) and [Supplementary Fig. 3](#)). Therefore, this observation led us to conclude that the decrease in the avoidance index at the end of the demyelination period was most likely due to a loss of visual acuity.

Visual avoidance correlates with drug-induced improved remyelination

Having shown the direct link between a failure or recovery of the visual avoidance index and a given demyelinated lesion or spontaneous myelin recovery of the optic nerve, respectively, we questioned whether this functional test could also apply to evaluate a

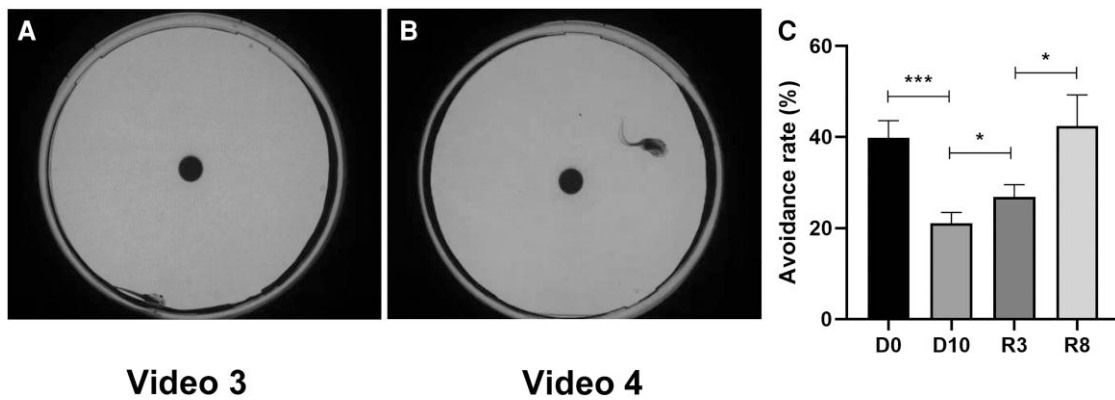


Figure 3 Live tracking of the visual avoidance paradigm. *Tg(mbp:GFP-NTR)* was recorded before (A and [Supplementary Video 3](#)) and at the end of 10 days of exposure to MTZ (end of demyelination period) (B and [Supplementary Video 4](#)). The ratio of the number of encounters that resulted in a successful avoidance allowed definition of an avoidance rate (C). Note that the sharp decrease in the avoidance index was not a consequence of an alteration of the swimming behaviour because demyelinated animals were still responding to a touch stimulus with a plastic pipette, as illustrated in [Supplementary Video 4](#) at 22 s.

drug-induced acceleration of remyelination. We have previously shown that among a panel of candidates favouring remyelination, clemastine and siponimod were the most efficient drugs to accelerate remyelination in our model of conditionally demyelinated tadpoles.¹⁵ It has been shown that in murine neonatal hypoxic injury clemastine promotes OPC differentiation and myelination, via an effect on the M1 muscarinic receptor on OPC.²⁰ Siponimod, a potent and highly selective sphingosine 1-phosphate receptor 1 and 5 (S1P1/5) modulator, has been shown to promote remyelination by a dual effect on both the innate immune system and maturation of oligodendrocytes.^{15,21} In the last series of experiments the number of GFP+ oligodendrocytes per optic nerve was counted before conditional demyelination, at the end of MTZ-induced demyelination and after 3 days of either spontaneous or clemastine- or siponimod-driven recovery ([Fig. 5A](#)). At R3 the number of GFP+ cells per optic nerve in tadpoles treated with clemastine (200 nM) was 1.5-fold higher (13.5 ± 0.3 , mean \pm SEM; $n = 13$) compared to control animals (8.8 ± 0.4 mean \pm SEM; $n = 13$; $P = 0.0003$). As expected, this clemastine-driven increase in remyelination translated into a functional improvement of all three behavioural assays: distance travelled was increased by 1.58-fold versus control (71.2 ± 6.7 cm versus 45.0 ± 5.8 cm), velocity by 1.58-fold (2.05 ± 0.19 cm/s versus 1.3 ± 0.17 cm/s) and visual avoidance index by 1.4-fold versus control ($76.6\% \pm 4.6\%$ versus $53.3\% \pm 6.4\%$) (mean \pm SEM, $n = 13$; [Fig. 5B–E](#), light grey columns). Treatment of demyelinated tadpoles with siponimod (3 nM) increased the number of GFP+ cells by a factor of 1.26 compared to control (10.7 ± 0.2 versus 8.5 ± 0.2 ; $n = 9$) and by 1.37-fold the visual avoidance index (75.0 ± 4.5 versus 54.5 ± 5.4 ; mean \pm SEM, $n = 9$). However, siponimod treatment did not result in a significant improvement of either average swimming speed or distance travelled ([Fig. 5B–E](#), dark grey columns). We had previously shown that in our *Xenopus* model of conditional de/remyelination, siramesine and sildenafil had no appreciable effect on remyelination.¹⁵ Siramesine (5 μ M) or sildenafil (1 μ M) were added for 3 days at the end of the demyelination process. We confirmed that neither siramesine nor sildenafil improved remyelination, evaluated by counting the number of GFP+ cells per optic nerve, and as expected, they had no significant effect on any of the three functional behavioural tests ([Fig. 5F–I](#)). Altogether these data confirm the usefulness of our conditional demyelination model to screen drugs for their potency to promote functional remyelination.

Discussion

Numerous drugs targeting the inflammatory component of multiple sclerosis are now available, some of them having a positive impact on disability progression.²² However, despite this therapeutic progress, there is still a need to find drugs that can halt silent progression, which correlates with chronic demyelination and related neurodegeneration. Loss of the myelin sheath perturbs normal axon functioning and persistent demyelination renders them vulnerable to irreversible damage leading to axonal transection, with consequent disability accumulation. It is established from experimental, neuropathological and imaging studies that remyelination is neuroprotective, although in most cases insufficient in multiple sclerosis, this remyelination failure being a key player of irreversible axonal damage and neuronal loss.²³ Several candidates based on promising efficacy in animal models have reached clinical trials but then failed. One possible reason for these failures is that, in most of the cases, during preclinical testing, efficacy was evaluated mostly on histology only, while behavioural improvement had not been experimented. A typical example is that screening procedures are often based on oligodendrocyte precursor cell proliferation and differentiation, events preceding and different from efficacious wrapping around axons, in as much as there is some evidence that these processes may be independently regulated.^{24,25} Keeping in mind that histopathological analysis does not allow us to ascertain the functional consequences of demyelination and recovery after remyelination,²⁶ we developed functional assays in the experimental model of conditional demyelination in *Xenopus*, our reasoning being that behavioural testing should bridge the gap between the evaluation criteria used in experimental models and clinical trials, therefore providing an alternative evaluation of preclinical therapeutic interventions. Here we have been using two types of functional testing: (i) distance travelled and speed of swimming evaluated motor behaviour, which can be compared to several motor tests developed in rodents, such as rotarod, pole tests, beam walking, open field tests, complex wheel, walking ladder, foot print; and (ii) avoidance of a virtual collision tested the visual system, which in rodent are evaluated by different approaches such as electroretinogram or optokinetic tracking or visual evoked potentials (VEP).

The rotarod is the most frequently used test for neuromotor performance in rodents. Developed more than 50 years ago,²⁷

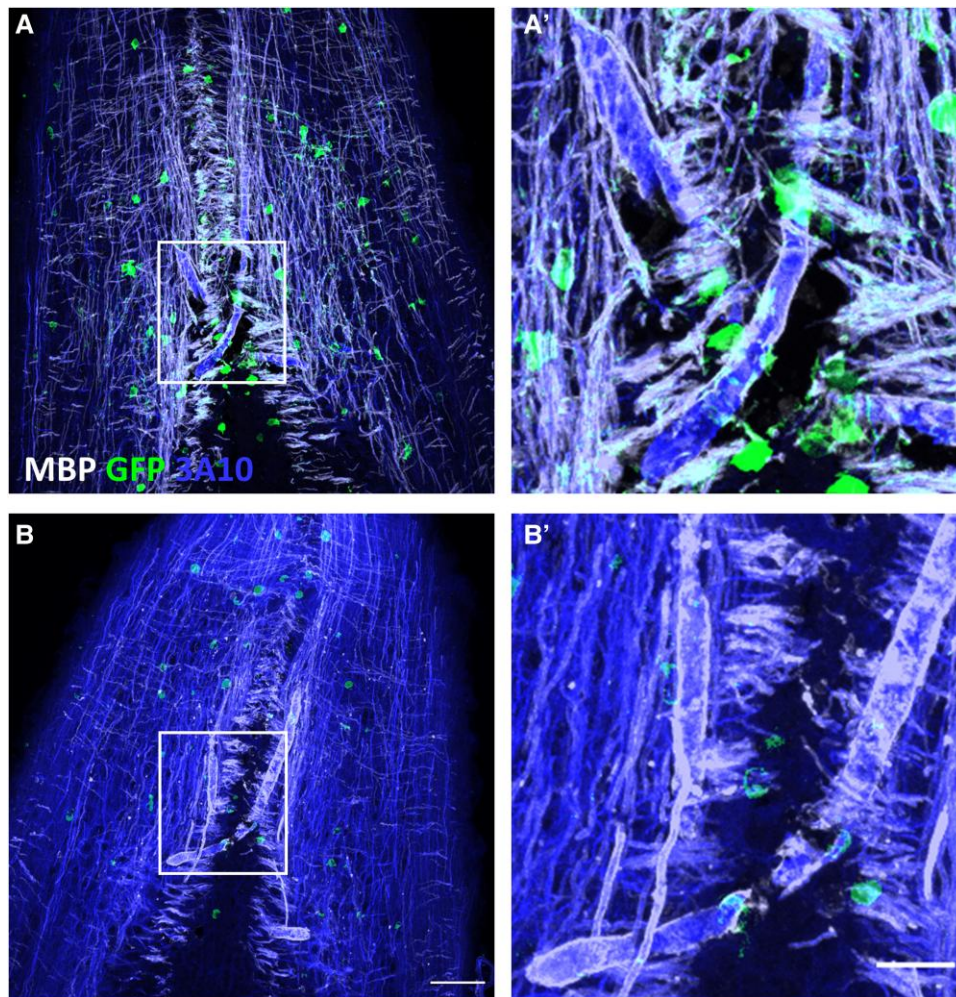


Figure 4 Immunostaining of brain stem at the level of Mauthner axons. Horizontal cryostat section of the brain stem of transgenic *Tg(mbp:GFP-NTR)* *Xenopus* tadpoles immunostained for GFP (mature oligodendrocytes), 3A10 (axons) and MBP (myelin sheath around axons) before demyelination (A) and at the end of MTZ exposure (B) causing ablation of about two-thirds of GFP+ oligodendrocytes. Demyelination in B is evidenced by loss of MBP staining around 3A10+ axons. However, demyelination is incomplete and notably the very large Mauthner axons (at higher magnification in A' and B') remained MBP positive. Scale bar = 50 μm (A and B) and 20 μm (A' and B').

it measures the ability of mice or rats to maintain balance on a rotating rod; therefore, it evaluates cerebellar function and motor coordination. The basic principle is the ability to hold and the general parameter measured is the latency to fall and number of flip/fall as illustrated in the cuprizone (CPZ)-induced demyelination/remyelination model.²⁸ In our *Xenopus* model, locomotion was tested by measuring the distance and the speed of swimming, two parameters significantly altered at the end of demyelination process and restored following remyelination. In rodents the distance travelled is more easily performed in the open field, which explores both locomotor activity and anxiety-like behaviour. In this test rodents are placed in a circular or square open environment and the total distance travelled and velocity are explored in addition to curiosity-like activities. Of note, data presented in the CPZ-induced demyelination model were inconsistent and contradictory; some reported that CPZ-treated mice spent more time with locomotion, their mean velocity was significantly higher and the distance they travelled was longer than untreated mice.^{29,30} In contrast, some authors reported that CPZ feeding significantly decreased distance moved and movement velocity compared to the control group,^{31,32} while others claimed the locomotor activity

data showed that the total distance travelled was similar in mice with CPZ treatment and control mice, suggesting intact motor function in the CPZ-treated animals.³³ These discrepancies may be due to the fact that demyelination-related impairment of locomotor activity may occur at different levels of the motor tracts and may not be simple to monitor.

In this respect, demyelination-induced visual impairment allows a more precise localization of demyelinated lesions. Visual disturbances are the most frequent initial manifestation of multiple sclerosis.³⁴ In rodents, demyelination of visual tracks are inferred when altered performances are measured in tests depending on visual cues, such as running wheel or the Y-maze.³⁵ More specific tests are also developed, such as multifocal electroretinograms³⁶ or quantification of mouse spatial vision using a virtual optomotor system.³⁷ In multiple sclerosis patients, demyelination of the optic nerve is most often associated with the loss of retinal ganglion cells, evaluated by optical coherence tomography, a technique well adapted to mouse and rats.²¹ VEP, i.e. visual system responses to repeated visual stimuli, allowed the latency and amplitude of a signal from the retina to the visual cortex to be recorded. VEP provides a tool to investigate signal processing through the visual system along the optic

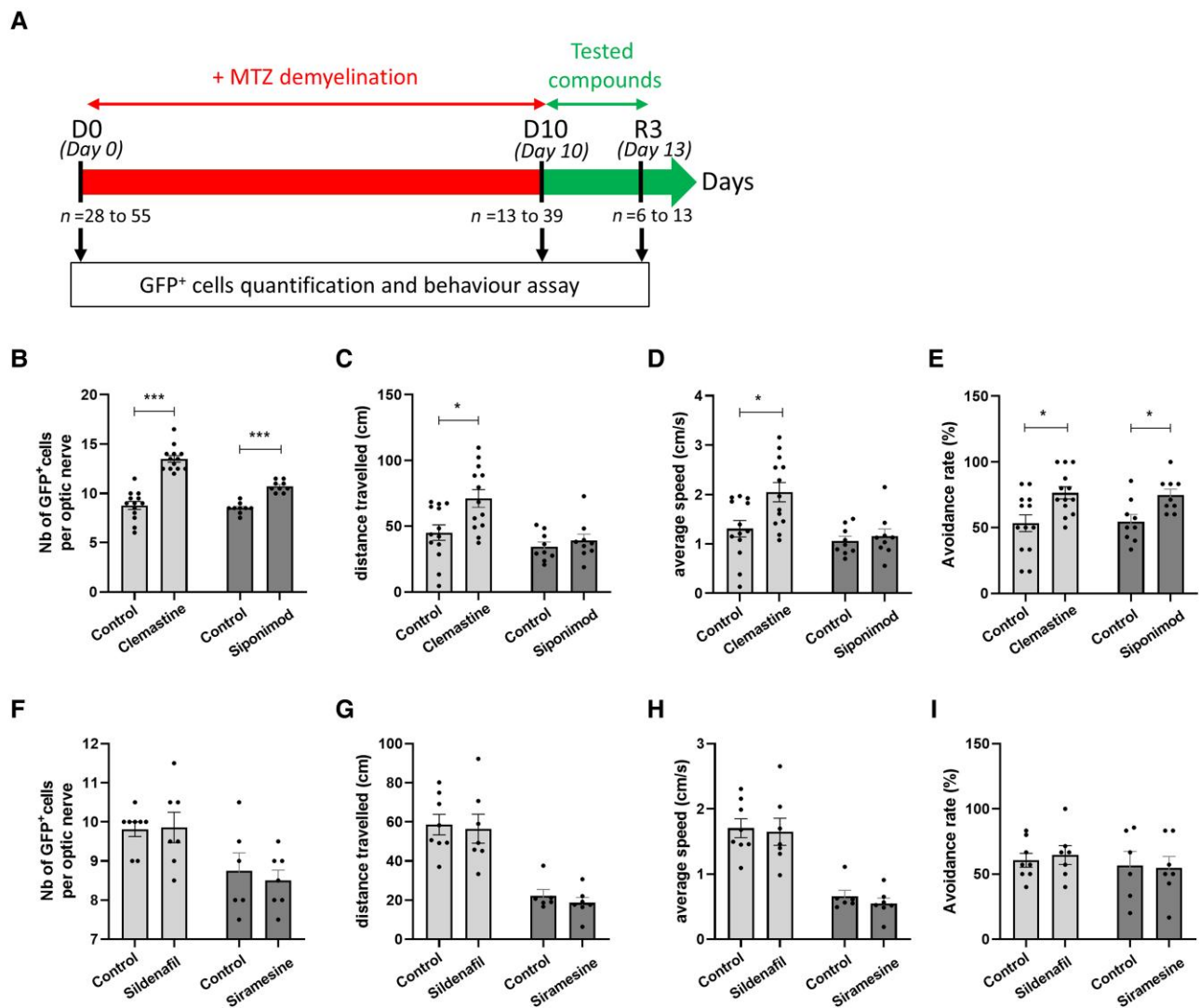


Figure 5 Improvement of visual avoidance index upon remyelination. Transgenic *Tg(mbp:GFP-NTR)* *Xenopus* tadpoles (stage 48–50) were treated for 10 days with metronidazole (10 mM) then returned to either fresh water (controls, Ctrl) or water containing the compound to be tested. Three days after the demyelination period (R3) tadpoles were first submitted to the visual avoidance test in the morning and in the afternoon the number of GFP+ cells per optic nerve was counted *in vivo*. (A) Flow chart showing the sequence of events tested and the number of tadpoles throughout the experiments. B–E show the results for clemastine (200 nM; light grey columns) and siponimod (3 nM; dark grey columns), two molecules which were shown to promote remyelination in our *Xenopus* model.¹⁵ Four parameters have been evaluated: number of GFP+ cells per optic nerve (B), distance travelled (in cm) during 30 s (C), average speed of swimming (in cm/s) (D) and avoidance index (E). F–I show the results for siramesine (5 μ M; light grey columns) and sildenafil (1 μ M; dark grey columns), two molecules that were previously tested as inefficient to promote remyelination.¹⁵ Neither siramesine nor sildenafil had any pro-remyelination effect either on number of GFP+ cells (F) or on any of the behaviour tests (G–I).

nerve and optic track, although lacking specificity about lesion location in the case of concomitant pre- and retrochiasmatic lesions.^{38–40}

In multiple sclerosis and optic neuritis, VEP tests are useful in detecting abnormality in patients, monitoring the progression of lesions, including remyelination, and correlating well with optical coherence tomography.^{41,42}

In this context, our transgenic model of conditional demyelination in which, thanks to the transparency of tadpoles, the extent of remyelination can be monitored *in vivo* and coupled to the restoration of function including a visual avoidance index, represents a reliable and simple assay to ascertain functional recovery after demyelination, therefore providing a way to de-risk and be predictive of the outcome of therapeutic trials targeting remyelination.

Acknowledgements

We are thankful to Dr Cheryl-Ann Friedman (McGill University) for helpful discussion on interspecies comparison of *mbp* regulatory sequences. Rabbit anti-pan neurofascin was a generous gift from Dr P.J. Brophy (University of Edinburgh); mouse monoclonal antibody IgG1 anti-neurofilament, clone 3A10, developed by Jessel/Dodd/Brenner-Morton, was obtained from the Developmental Studies Hybridoma Bank, developed under the auspices of the NICDH and maintained by the University of Iowa, Department of Biology, Iowa City, IA, USA (52 242). We thank David Akbar and ICM-QUANT imaging facility for help in generating micrograph illustrations.

Funding

Our laboratory is supported by Inserm, CNRS, Sorbonne University, Paris Brain Institute (ICM), the program 'Investissements d'avenir' programs ANR-10-IAIHU-06 (IHU-A-ICM) and NeurATRIS. The study was partially funded by research grants to BZ from the European Union's Horizon 2020 Research and Innovation Program ENDpoiNTs project Grant Agreement number: 825759, grant BRECOMY funded jointly by DFG and ANR, grant MADONA from ANSES and grant IONESCO from NeurATRIS.

Competing interests

The authors report no competing interests.

Supplementary material

Supplementary material is available at *Brain* online.

References

1. Bechler ME, Byrne L, Ffrench-Constant C. CNS myelin sheath lengths are an intrinsic property of oligodendrocytes. *Curr Biol*. 2015;25:2411-2416.
2. Ranvier L. *Leçons Sur l'histologie Du Système Nerveux. Recueillies Par Ed Weber*. Savy. 1878; 131.
3. Fünfschilling U, Supplie LM, Mahad D, et al. Glycolytic oligodendrocytes maintain myelin and long-term axonal integrity. *Nature*. 2012;485:517-521.
4. Lee Y, Morrison BM, Li Y, et al. Oligodendroglia metabolically support axons and contribute to neurodegeneration. *Nature*. 2012;487:443-448.
5. Bjartmar C, Trapp BD. Axonal and neuronal degeneration in multiple sclerosis: Mechanisms and functional consequences. *Curr Opin Neurol*. 2001;14:271-278.
6. Kaya F, Mannioui A, Chesneau A, et al. Live imaging of targeted cell ablation in *Xenopus*: A new model to study demyelination and repair. *J Neurosci*. 2012;32:12885-12895.
7. Dong W, Lee RH, Xu H, et al. Visual avoidance in *Xenopus* tadpoles is correlated with the maturation of visual responses in the optic tectum. *J Neurophysiol*. 2009;101:803-815.
8. Khakhalin AS, Koren D, Gu J, Xu H, Aizenman CD. Excitation and inhibition in recurrent networks mediate collision avoidance in *Xenopus* tadpoles. *Eur J Neurosci*. 2014;40:2948-2962.
9. Nieuwkoop PD, Faber J. *Normal Table of Xenopus laevis (Daudin)*. Garland; 1994.
10. Green AJ, Gelfand JM, Cree BA, et al. Clemastine fumarate as a remyelinating therapy for multiple sclerosis (ReBUILD): A randomised, controlled, double-blind, crossover trial. *Lancet*. 2017;390:2481-2489.
11. Zonta B, Tait S, Melrose S, et al. Glial and neuronal isoforms of neurofascin have distinct roles in the assembly of nodes of Ranvier in the central nervous system. *J Cell Biol*. 2008;181:1169-1177.
12. Stankoff B, Demerens C, Goujet-Zalc C, et al. Transcription of myelin basic protein promoted by regulatory elements in the proximal 5' sequence requires myelinogenesis. *Mult Scler*. 1996;2:125-132.
13. Farhadi HF, Lepage P, Forghani R, et al. A combinatorial network of evolutionarily conserved myelin basic protein regulatory sequences confers distinct glial-specific phenotypes. *J Neurosci*. 2003;23:10214-10223.
14. Gow A, Friedrich VL, Lazzarini RA. Myelin basic protein gene contains separate enhancers for oligodendrocyte and Schwann cell expression. *J Cell Biol*. 1992;119:605-616.
15. Mannioui A, Vauzanges Q, Fini JB, et al. The *Xenopus* tadpole: An *in vivo* model to screen drugs favoring remyelination. *Mult Scler*. 2018;24:1421-1432.
16. Khakhalin AS. Analysis of visual collision avoidance in *Xenopus* tadpoles. *Cold Spring Harb Protoc*. 2021; 2021:4.
17. Liu Z, Hamodi AS, Pratt KG. Early development and function of the *Xenopus* tadpole retinotectal circuit. *Curr Opin Neurobiol*. 2016;41:17-23.
18. Korn H, Faber DS. The Mauthner cell half a century later: A neurobiological model for decision-making? *Neuron*. 2005;47:13-28.
19. Zottoli SJ, Hordes AR, Faber DS. Localization of optic tectal input to the ventral dendrite of the goldfish Mauthner cell. *Brain Res*. 1987;401:113-121.
20. Cree BAC, Niu J, Hoi KK, et al. Clemastine rescues myelination defects and promotes functional recovery in hypoxic brain injury. *Brain*. 2018;141:85-98.
21. Dietrich M, Hecker C, Hilla A, et al. Using optical coherence tomography and optokinetic response as structural and functional visual system readouts in mice and rats. *J Vis Exp*. 2019;143:e58571.
22. Hauser SL, Cree BAC. Treatment of multiple sclerosis: A review. *Am J Med*. 2020;133:1380-1390.e2.
23. Lubetzki C, Zalc B, Williams A, Stadelmann C, Stankoff B. Remyelination in multiple sclerosis: From basic science to clinical translation. *Lancet Neurol*. 2020;19:678-688.
24. Xin W, Chan JR. Myelin plasticity: Sculpting circuits in learning and memory. *Nat Rev Neurosci*. 2020;21:682-694.
25. Zhou X, He C, Ren J, et al. Mature myelin maintenance requires pki to coactivate PPAR β -RXR α -mediated lipid metabolism. *J Clin Invest*. 2020;130:2220-2236.
26. Crawford DK, Mangiardi M, Tiwari-Woodruff SK. Assaying the functional effects of demyelination and remyelination: Revisiting field potential recordings. *J Neurosci Methods*. 2009;182:25-33.
27. Jones BJ, Roberts DJ. The quantitative measurement of motor inco-ordination in naive mice using an accelerating rotarod. *J Pharm Pharmacol*. 1968;20:302-304.
28. Franco-Pons N, Torrente M, Colomina MT, Vilella E. Behavioral deficits in the cuprizone-induced murine model of demyelination/remyelination. *Toxicol Lett*. 2007;169:205-213.
29. Bölcskei K, Kriszta G, Sághy É, et al. Behavioral alterations and morphological changes are attenuated by the lack of TRPA1 receptors in the cuprizone-induced demyelination model in mice. *J Neuroimmunol*. 2018;320:1-10.
30. Shao Y, Peng H, Huang Q, Kong J, Xu H. Quetiapine mitigates the neuroinflammation and oligodendrocyte loss in the brain of C57BL/6 mouse following cuprizone exposure for one week. *Eur J Pharmacol*. 2015;765:249-257.
31. Vakilzadeh G, Khodaghali F, Ghadiri T, et al. The effect of melatonin on behavioral, molecular, and histopathological changes in cuprizone model of demyelination. *Mol Neurobiol*. 2016;53:4675-4684.
32. Mitra NK, Xuan KY, Teo CC, Xian-Zhuang N, Singh A, Chellian J. Evaluation of neuroprotective effects of alpha-tocopherol in cuprizone-induced demyelination model of multiple sclerosis. *Res Pharm Sci*. 2020;15:602-611.
33. Wang H, Li C, Wang H, et al. Cuprizone-induced demyelination in mice: Age-related vulnerability and exploratory behavior deficit. *Neurosci Bull*. 2013;29:251-259.
34. Confavreux C, Vukusic S, Adeleine P. Early clinical predictors and progression of irreversible disability in multiple sclerosis: An amnesic process. *Brain*. 2003;126(Pt 4):770-782.

35. Sen MK, Mahns DA, Coorsen JR, Shortland PJ. Behavioral phenotypes in the cuprizone model of central nervous system demyelination. *Neurosci Biobehav Rev.* 2019;107:23-46.
36. Dutescu RM, Skosyrski S, Kociok N, et al. Multifocal ERG recordings under visual control of the stimulated fundus in mice. *Invest Ophthalmol Vis Sci.* 2013;54:2582-2589.
37. Prusky GT, Alam NM, Beekman S, Douglas RM. Rapid quantification of adult and developing mouse spatial vision using a virtual optomotor system. *Invest Ophthalmol Vis Sci.* 2004;45:4611-4616.
38. Castoldi V, Marenga S, d'Isa R, et al. Non-invasive visual evoked potentials to assess optic nerve involvement in the dark agouti rat model of experimental autoimmune encephalomyelitis induced by myelin oligodendrocyte glycoprotein. *Brain Pathol.* 2020;30:137-150.
39. Ridder WH, Nusinowitz S. The visual evoked potential in the mouse—Origins and response characteristics. *Vision Res.* 2006;46(6–7):902-913.
40. Strain GM, Tedford BL. Flash and pattern reversal visual evoked potentials in C57BL/6J and B6CBAF1/J mice. *Brain Res Bull.* 1993;32:57-63.
41. Pihl-Jensen G, Wanscher B, Frederiksen JL. Predictive value of optical coherence tomography, multifocal visual evoked potentials, and full-field visual evoked potentials of the fellow, non-symptomatic eye for subsequent multiple sclerosis development in patients with acute optic neuritis. *Mult Scler.* 2021;27:391-400.
42. Zafeiropoulos P, Katsanos A, Kitsos G, Stefanidou M, Asproudis I. The contribution of multifocal visual evoked potentials in patients with optic neuritis and multiple sclerosis: A review. *Doc Ophthalmol.* 2021;142:283-292.